Eur. Phys. J. B **12**, 39–46 (1999)

THE EUROPEAN PHYSICAL JOURNAL B

EDP Sciences

Dipolar interaction and incoherent quantum tunneling: a Monte Carlo study of magnetic relaxation

A. Cuccoli[1,a], A. Fort[2], A. Rettori[1], E. Adam[3], and J. Villain[3,4]

[1] Dipartimento di Fisica dell'Università di Firenze and Istituto Nazionale di Fisica della Materia, Largo E. Fermi 2, 50125 Firenze, Italy
[2] Istituto di Elettronica Quantistica del CNR Via Panciatichi 56/30, 50127 Firenze, Italy
[3] Département de Recherche Fondamentale sur la Matière Condensée, CEA Grenoble, 17 avenue des Martyrs, 38054 Grenoble Cedex 9, France
[4] CRTBT, CNRS, B.P. 166, 38042 Grenoble Cedex 9, France

Received 9 February 1999

Abstract. We study the magnetic relaxation of a system of localized spins interacting through weak dipole interactions, at a temperature large with respect to the ordering temperature but low with respect to the crystal field level splitting. The relaxation results from quantum spin tunneling but is only allowed on sites where the dipole field is very small. At low times, the magnetization decrease is proportional to $\sqrt{t}$ as predicted by Prokofiev and Stamp, and at long times the relaxation can be described as an extension of a relaxed zone. The results can be directly compared with very recent experimental data on Fe_8 molecular clusters.

PACS. 75.45.+j Macroscopic quantum phenomena in magnetic systems – 75.40.Mg Numerical simulation studies – 75.50.Xx Molecular magnets – 61.46.+w Clusters, nanoparticles, and nanocrystalline materials

1 A novel relaxation mechanism

The relaxation of a quantity $m(t)$ toward its equilibrium value $m(\infty)$ is usually described by a standard model taken from a surprisingly limited set, in contrast with the extreme diversity of the physical problems to which each of these models apply. The simplest model is the linear equation

$$\frac{\mathrm{d}m(t)}{\mathrm{d}t} = -\alpha[m(t) - m(\infty)] \tag{1}$$

where α is a constant.

The compound $[(\mathrm{tacn})_8\mathrm{Fe}_8\mathrm{O}_8(\mathrm{OH})_8]^{8+}$ (where tacn is 1-4-7-triazacyclononane) pertains, at low temperature T < 1 K, to a new class which has not been studied until very recently [1,2]. This material [3], hereafter called "Fe_8", is a paramagnet and the quantity $m(t)$ of interest is the magnetization per spin, more precisely its component along a well defined axis z which is an easy magnetization axis. According to current knowledge [3], this material is made of molecular groups, each of which contains 8 ions Fe^{+++} and has at low temperature a spin $s = 10$ which results from a strong exchange coupling between the 8 Fe^{+++} ions. At low temperature each molecular spin $\boldsymbol{S}_i$ is oriented along z, with the value

$$S_i^z = S_i = \pm s. \tag{2}$$

The weak dipole interaction between different molecular groups is not sufficient to produce a magnetic order at any accessible temperature and, at thermal equilibrium, the $+s$ and $-s$ spins are randomly distributed with an average value $m(\infty)$ which depends on the external field. In a typical relaxation experiment at very low temperature, all spins are initially in the state

$$S_i^z(0) = -s \tag{3}$$

so that $m(0) = -s$.

Above 1 K, the relaxation is well described by (1) and the relaxation is exponential [3],

$$m(t) - m(\infty) = [m(0) - m(\infty)]\exp(-t/\tau). \tag{4}$$

However, at low temperature, the relaxation is not exponential. At long times t, it is pretty well described by a stretched exponential [3]

$$m(t) - m(\infty) = [m(0) - m(\infty)]\exp[-(t/\tau)^{\beta_1}] \tag{5}$$

where the exponent β_1 depends on T and takes the value 1 above 1 K. Below 0.4 K, β_1 is nearly constant [3] and equal to

$$\beta_1 \approx 0.4. \tag{6}$$

[a] e-mail: cuccoli@fi.infn.it

In the present work, kinetic Monte Carlo simulations of the magnetic relaxation of Fe_8 are reported; they are made on the basis of a model described in the next section.

2 The incoherent tunneling model

At the low temperatures of interest, thermal activation is impossible and the relaxation takes place by tunneling. In weak external field, tunneling takes place between the two states (2), and is only possible for a spin $\boldsymbol{S}_i$ if the z-component H_i of the local magnetic field is very close to 0, say

$$-H_1 < H_i < H_1 \tag{7}$$

where H_1 is a constant which will be precised below. The local field is the sum of the external field $H_{\rm ext}$ and an internal field. In most of materials, the internal field is partly due to nuclear spins (hyperfine interactions). When the magnetic particles are Fe, the hyperfine contact interaction is nearly absent because the most common Fe isotope has no spin, the magnetic isotope has a weak concentration (2%) and moreover a weak spin (1/2). In the present work, hyperfine interactions will not be explicitly taken into account in the evaluation of the internal field. They are but implicitly included in the theory since they are probably [1,2] responsible for the resonance width H_1. This width has been measured by Wernsdorfer *et al.* [4] in Fe_8 and is of order 10 Oersteds.

Thus, the internal field only depends on the molecular spins through the formula

$$H_{\rm dip}^{(i)} = \sum_j g_{ij} S_j. \tag{8}$$

This field will hereafter be called "dipole field" although it may also contain an exchange component. At long distance this exchange part vanishes and the coefficients $g_{ij} = g(\boldsymbol{r}_i - \boldsymbol{r}_j)$ behave according to the formula

$$g(\boldsymbol{r}) = -\frac{K}{r^3}\left(1 - 3z^2/r^2\right) \tag{9}$$

where z is the component of $\boldsymbol{r}$ on the z axis.

In a finite system, tunneling is an undamped oscillation between two states and does not really result in relaxation. For instance, if the spin $\mathbf{S}_i$ were isolated, it would oscillate in zero field between the two states (2). This is not true for the large systems which are studied in experimental physics, and it is reasonable to make the following assumption.

Basic assumption

Any spin i subject to a local field H_i has a probability $\eta(H_i)$ per unit time of transition between the two states (2). The real, nonnegative function $\eta(H_i)$ is negligible if H_i does not satisfy (7).

The choice of the function $\eta(H)$ is presumably not essential provided the above properties are satisfied. A possible choice is

$$\begin{cases} \eta(H)=\eta(0)\left[1-\dfrac{H^2}{H_1^2}\right] & (-H_1 < H < H_1) \\ \eta(H)=0 & (|H| > H_1). \end{cases} \tag{10}$$

The above assumption defines the "incoherent tunneling model" which is studied in the next sections. Since the spin-flip transitions modify the fields, the relaxation defined by the basic assumptions and by formula (8) is difficult. It has been investigated by kinetic Monte Carlo simulations by Prokofiev and Stamp [1] and by Ohm and Paulsen [5]. More detailed results are presented in Section 6. They include a detailed analysis of the effect of the sample shape and crystal structure.

Prokofiev and Stamp have given an analytic description of the short time behavior. A critical summary of this theory is given in the next section.

In higher external field, the basic assumption must be modified since tunneling becomes possible from state $S_z^i = -s$ to an eigenstate (or rather, nearly eigenstate) $S_z^i = m$, with $0 < m < s$, if the external field is such that two eigenvectors of the spin Hamiltonian have nearly the same energy (resonance condition) [6]. Then, the spin emits phonons and goes to state $S_z^i = s$. It would be easy to include this possibility in the following calculations, but for the sake of simplicity it will be ignored. This is correct if the external field is not too large.

3 The Prokofiev-Stamp approximation for a sphere

Since the dipole interactions (8) are essential in the model, the shape of the sample should be important if the model is correct. The simplest case is that of a spherical sample. Then (3) implies, at $t = 0$, that the local field H_i has the same value $H(0)$ for all spins i, *except* near the surface.

It will be assumed in this section that the sample is spherical and that the external field is such that $H(0) = 0$. These conditions allow the rapid reversal of a certain amount of spins. Because of this process, the local field is no longer uniform, so that the reversal of most of the other spins is hindered. The distribution $P(t;H)$ of the local fields at time t will be assumed to be continuous, and the proportion of spins which can reverse in the time unit is of order $\eta(0)H_1P(t;0)$; this value is exact if $\eta(H) = \text{const.}$ in a range of width H_1 and zero outside. If one assumes that the local field H_i and the spin S_i are independent at each time, it follows from equation (10)

$$\frac{\mathrm{d}}{\mathrm{d}t}m(t) = -\frac{4}{3}\eta(0)H_1P(t;0)m(t). \tag{11}$$

The function $P(t;H)$ is characterized by its width $\Gamma(t)$, so that (11) can be replaced by

$$\frac{\mathrm{d}}{\mathrm{d}t}m(t) = -\frac{4}{3}\eta(0)H_1m(t)/\Gamma(t). \tag{12}$$

In order to obtain a closed evolution equation for $m(t)$, one should relate $\Gamma(t)$ to the magnetization $m(t)$.

When m has its saturation value $-s$, as is the case at $t = 0$, the width Γ vanishes for a spherical sample. According to Prokofiev and Stamp, $\Gamma(t) = \Gamma(m(t))$ with

$$\Gamma(m) = (1 - |m|/s)H_{\rm d} \tag{13}$$

where the constant $H_{\rm d}$ has the order of magnitude of the maximum dipole field.

Relation (13) can be justified as follows. At short times, the local field is the sum of the initial field, which has been assumed to be 0, and the dipole field produced by those spins which are already reversed. Let ℓ be the average distance between those spins. The typical value of the resulting dipole field, as given by (9), is of order $K/\ell^3 \approx H_{\rm d}a^3/\ell^3$, where a is the distance between spins. The width $\Gamma(m)$ should have the same order of magnitude, $\Gamma(m) \approx H_{\rm d}a^3/\ell^3$. Now, a^3/ℓ^3 is the proportion of reversed spins, *i.e.* $(1 - |m|/s)/2$. Relation (13) follows.

Insertion of (13) into (12) yields

$$[1-|m(t)|/s]\frac{\rm d}{{\rm d}t}[1-|m(t)|/s] \approx \eta(0)H_1|m(t)|/(sH_{\rm d}) \tag{14}$$

the solution of which is

$$\eta(0)H_1 t/H_{\rm d} \approx |m(t)|/s - 1 - \ln[|m(t)|/s]. \tag{15}$$

For short times, (15) reduces to the result of Prokofiev and Stamp [1]

$$1 - |m(t)|/s \approx \sqrt{t/\tau_a} \tag{16}$$

while, for long times, (15) reduces to

$$|m(t)|/s \approx \exp\left[-\frac{t}{\tau_a} - 1\right] \tag{17}$$

where

$$\tau_a = \frac{H_{\rm d}}{\eta(0)H_1}. \tag{18}$$

Formula (16) will be seen to describe correctly the short time behaviour, while the long time behaviour will be seen to be described by (5). Formulae (15, 17) will be seen not to be satisfactory at long times. This remark shows that the approximations made in the derivation of (16) are only valid at short times.

4 Non-resonant fields and non-spherical samples

The analytic formulae (15–17) have been obtained for a spherical sample when the external field is such that, at $t = 0$, the "resonance condition" $H_i = 0$ is satisfied for all spins i.

If in (8) the sum is replaced by an integral, the local field is uniform in a spherical sample, and vanishes exactly at saturation (*i.e.* if $S_i = -s$) if the external field is absent. However, the replacement by an integral is not exact, and the local field is not uniform at saturation, although it is very sharply peaked (Fig. 1a). As a matter of fact, it is

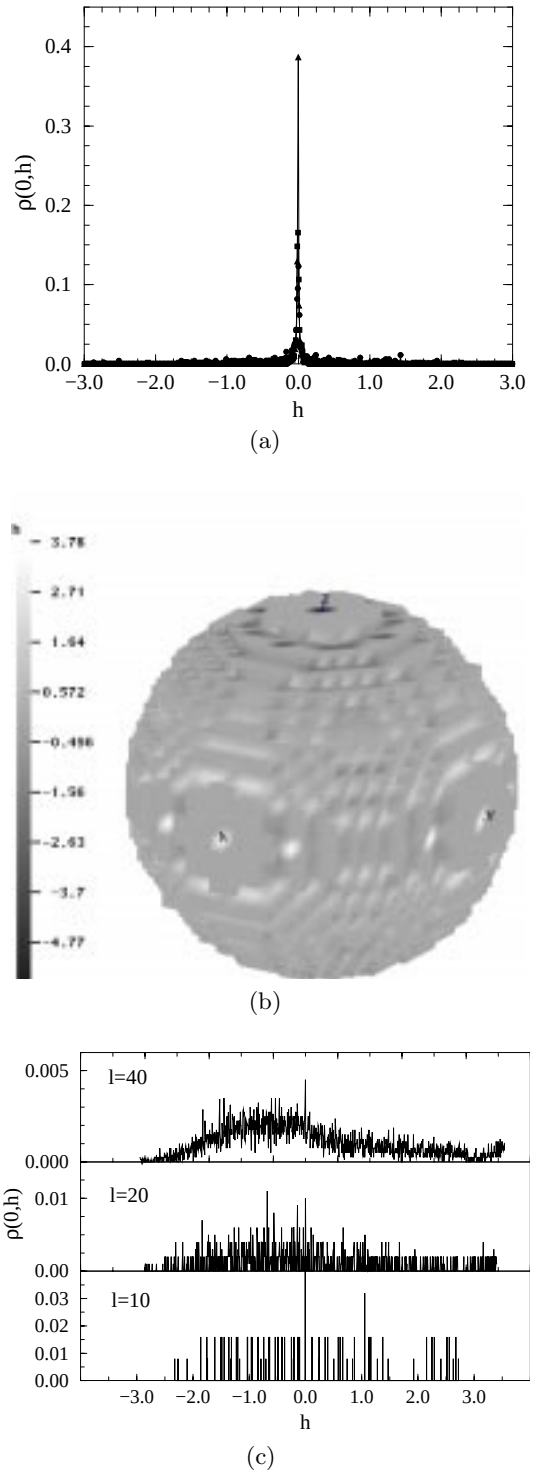

Fig. 1. Distribution of local fields at the sites of a simple cubic lattice occupied by spins parallel to the z axis. (a) Sphere of 9134 spins. The wings are due to the surface, as shown in picture (b). In such picture the clear regions are those where the local field is larger than its average value, the dark regions are those where it is lower. (c) Cube of different sizes: $10\times10\times10$, $20\times20\times20$, and $40\times40\times40$ spins, starting from below. The field is measured in units $g\mu_{\rm B}S/a^3$ ($\simeq 80$ Oersted, setting $S = 10$ and $a \simeq 13$ Å, average distance among Fe_8 clusters in the actual compound). Note as the size of the sample affects the discretization of the field values.

impossible to cut a perfect sphere in a crystalline material, and the edges can only be approximately spherical [7].

Relaxation can thus occur near the surface even if the resonance condition $H_i = 0$ is not satisfied in the bulk. The relaxation can propagate and possibly become total as $t \to \infty$. Whether this occurs or not is one of the questions to be answered by the simulations reported below.

If the sample is not a sphere (nor an ellipsoid) the resonance condition can only be satisfied in a part of the sample, even at $t = 0$, when $S_i = -s$ (Fig. 2b) so that the local field has a broad distribution (Figs. 1c, 2a). According to Prokofiev and Stamp [1], the variation of the magnetization at short time t is still proportional to $\sqrt{t/\tau}$ as in (16); such prediction has recently received beautiful experimental confirmations [4,5]. Moreover in reference [1] is found that the short time relaxation constant τ contains the volume where the local field has its resonance value. This prediction ignores the possible extension of this volume in time, and is therefore somewhat speculative, but it opens the possibility to experimentally probe the field distribution [4].

For a non-spherical sample, the square root law is observed on a broader field interval since the field distribution is broader. Moreover, the square root law can be generalized to any value of the initial magnetization namely [4]

$$m(0) - m(t) \approx \text{const.}\sqrt{t}. \tag{19}$$

This result holds only if the density of the local field does not change much for a field variation of the order of the resonance width H_1. This excludes spherical samples.

Some of the formulae written in Section 3 for a spherical sample can be generalized. For instance, if one introduces the local magnetization $m(\boldsymbol{r}, t)$ and the local distribution $P(\boldsymbol{r}, t; H)$ of internal field, (11) can be generalized as

$$\frac{\partial}{\partial t} m(\boldsymbol{r}, t) = -\frac{4}{3}\eta(0) H_1 P(\boldsymbol{r}, t; 0) m(\boldsymbol{r}, t). \tag{20}$$

Integrating $P(\boldsymbol{r}, t; H)$ on $\boldsymbol{r}$, one obtains the distribution of local fields at time t,

$$\rho(t; H) = \int \mathrm{d}^3 r \int_{-\infty}^{\infty} \mathrm{d}H' P(\boldsymbol{r}, t; H) \delta(H' - H) \tag{21}$$

which is shown for $t = 0$ for various sample shapes on Figures 1, 2 and 3.

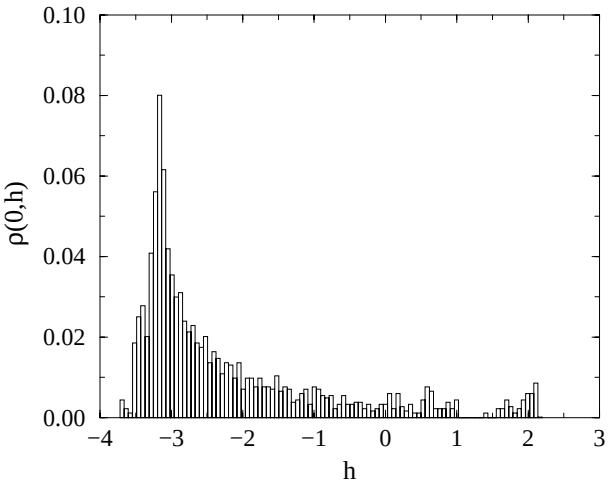

(a)

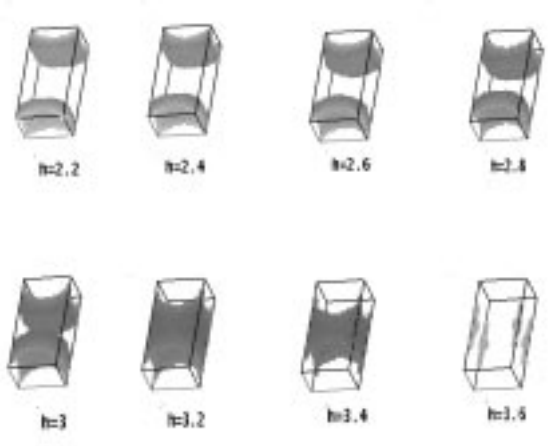

(b)

Fig. 2. (a) Distribution of local fields at the sites of a simple cubic lattice occupied by spins parallel to the z axis for a parallelepiped of $12 \times 17 \times 36$ spins. (b) The local fields through this sample: below each picture is reported the value of the external field to be applied to bring the shaded spins to resonance (the local field is given in units $g\mu_{\mathrm{B}} S/a^3 \simeq 80$ Oersted, see text in Sect. 5).

5 Monte Carlo simulations: model and method

The model sketched in Section 2 is not yet completely defined. The crystal lattice, for instance, has not been defined.

The material Fe_8 has a complicated, triclinic crystal structure. It can be taken into account in the simulations, but this does not warrant realism. A complete, realistic calculation would imply a calculation of the coefficients g_{ij} taking into account the exact shape of the electronic wave functions. This would be a difficult task. Moreover, the presence of short range exchange interactions, which would be more difficult yet to calculate, cannot be excluded.

We believe that all these unknown effects can be taken into account by a single parameter, which is the value H_0 of the external field at resonance for a sphere or at the center of a cube. For a cubic sample of a cubic crystal, $H_0 = 0$ by symmetry. For the real material Fe_8, H_0 does not vanish, cannot be calculated for the reasons explained above, but can easily be measured. When it is known, the field distribution in a sample of any shape can be calculated for a cubic lattice, and then obtained

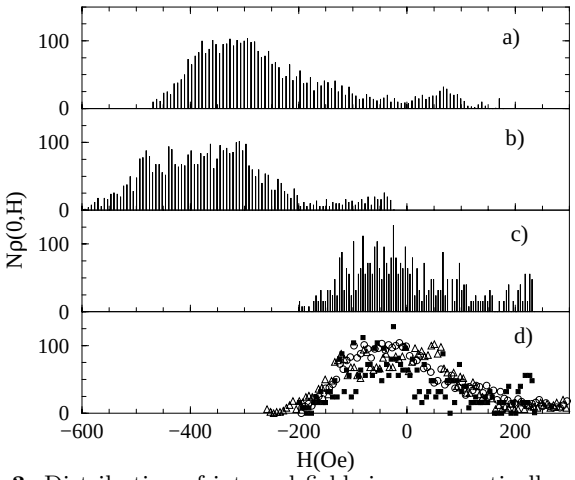

Fig. 3. Distribution of internal fields in a magnetically saturated sample of cubic shape. a) Spins localized at the Fe-ions sites of the actual material, ignoring the actual electronic density. b) Single giant spins localized at the sites of a triclinic lattice with the unit cell parameters of Fe_8. c) Single giant spins localized at the sites of a cubic lattice with lattice constant $a = 13$ Å. d) The same distributions given in the previous picture, with a) (open squares) and b) (open triangles) shifted by 280 and 360 Oersted, respectively.

for the real material by shifting the field scale by an amount H_0. The above views are supported by Figure 3 which shows the internal field distribution for a cubic lattice compared to other possible models. The distributions are not very different apart from a shift.

Most of our simulations have been performed on a cubic lattice. We have done a single simulation on a system with the crystal structure of Fe_8 (but with localized spins) and checked that there is no significant difference with simulations on a cubic lattice.

An important parameter is the resonance width H_1. If it were larger than $H_{\rm dip}$, the relaxation would be fast and exponential. The experimentally observed, slow relaxation is certainly related to a small value of H_1. In the simulations, H_1 cannot be smaller than the typical distance between the discrete values of the dipole field, which has a lower limit since the sample cannot be very large (see Fig. 1c); however, the sample dimension in our simulation allows us to employ a value of H_1 of the same order of magnitude of that deducible from experiments. In evaluating the local field we add to the dipolar contribution given by equations (8, 9) a constant, external, applied field which can be varied. In most of the figures reporting results of simulations we use the reduced field $h = H/\overline{H}$, where $\overline{H} = g\mu_{\rm B}S/a^3 \simeq 80$ Oersted, for $S = 10$ and $a = 13$ Å.

The Monte Carlo algorithm employed to simulate the dynamics of our systems is an implementation of those proposed and discussed elsewhere [8,9].

We start from a completely magnetized sample at time $t = 0$, and we evaluate the local field H_i acting on any site i of the lattice; we then cycle through the following steps:

i) We single out those sites where $|H_i| \leq H_1$; let us denote with n_0 the number of such spins which, according to our model, can relax with a probability given by equation (10). *ii)* We increment time replacing t by $t + \Delta t$, where Δt is chosen stochastically with probability $\eta_0 n_0 e^{-\eta_0 n_0 \Delta t}$, *i.e.* we set $\Delta t = -\ln\xi/(\eta_0 n_0)$, where ξ is a generated number uniformly distributed in $(0, 1)$. *iii)* We randomly choose one of those n_0 spins singled out in step *i)* and flip it with probability given by equation (10). *iii$_a$)* If the spin has been flipped we update the total magnetization and the fields on all sites of the lattice. *iv)* We come back to step *i)*.

For any set of the simulation parameters different independent runs were made and averaged. Some sample runs where also done using the more elementary algorithm which uses constant time steps; the results obtained are the same, but it takes much longer time, due to the smallness of the time step to be used to get stable results.

6 Monte Carlo simulations: results

6.1 Short time behavior

6.1.1 Spherical samples

For a spherical sample, the Prokofiev-Stamp formula (16) is very well satisfied if the uniform, initial local field $H(0)$ is smaller than the width H_1 (Fig. 4). For those fields, the agreement with (16) is good (except at very short times) as long as the magnetization is larger than 80% of its initial value. At extremely short times, the magnetization decays linearly with t as well known [1]. This can be understood because the spins relax independently since the average distance between reversed spins is very large and the dipole field created by the reversed spins is smaller than the width H_1.

Away from the resonance, *i.e.* for $H(0) = H > H_1$, formula (16) is no longer satisfied. However, if the initial field is not too far from the resonance, the magnetization becomes a linear function of $\sqrt{t}$ after a certain time $\tau_1(H)$. This phenomenon can presumably be interpreted as follows. For short times, $P(\boldsymbol{r}, t; 0) = 0$ except near the surface, so that $\partial m/\partial t$ is small according to equation (20). However, a partly relaxed zone, with $P(\boldsymbol{r}, t; 0) \neq 0$, will progressively invade the whole sample. The invasion is total at time $\tau_1(H)$. This time can be expected to become very long for big samples.

6.1.2 Parallelepipedic samples

We investigated an elongated, parallelepipedic sample whose shape ($12 \times 17 \times 36$ spins) roughly corresponds to that which was experimentally measured [3]. The Prokofiev-Stamp prediction (19) is satisfied for short times as shown by Figure 5. However, these "short" times are differently short for different external fields. For certain field values, the slope $|{\rm d}m/{\rm d}\sqrt{t}|$ suddenly decreases after a rather short time and the magnetization curve crosses other magnetization curves which satisfy the Prokofiev-Stamp prediction on a longer interval. This crossing has

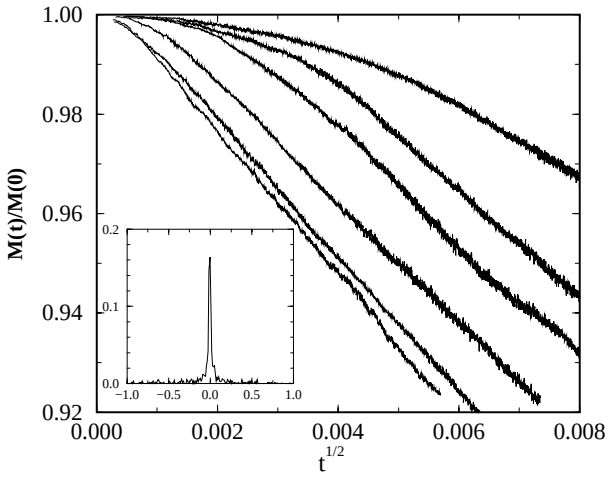

Fig. 4. Magnetization as a function of the square root of the time for a spherical sample of radius 13 lattice constants for $\eta(0) = 10^4$ and various applied fields h. From the uppermost curve: h=0.3, h=0.2, h=0.15, h=0.1, h=0.05, h=0. The reported data are the average over 10 independent runs. In the inset the field distribution is reported.

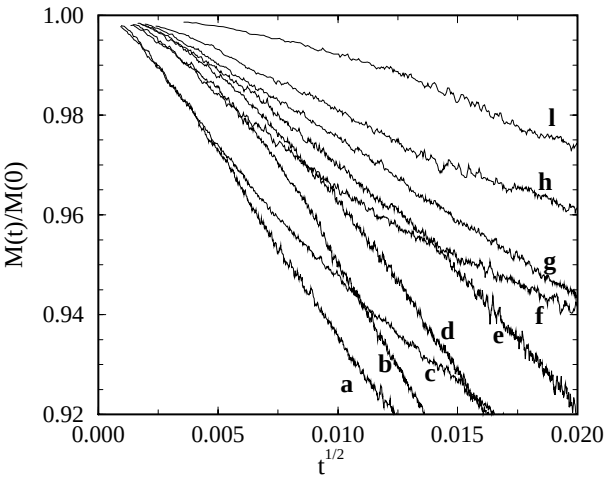

Fig. 5. Magnetization as a function of the square root of the time for a parallelepipedic sample of $12 \times 17 \times 36$ spins for $\eta(0) = 10^4$; the longest side is along the easy magnetization axis. The various curves correspond to the following applied fields: a) h=3; b) h=2.6; c) h=3.2; d) h=2.4; e) h=2.2; f) h=3.4; g) h=2; h) h=1.6; l) h=3.6. The reported data are the average over 10 independent runs.

not been experimentally seen. It is of interest to relate the different shapes of the demagnetization curve to the initial internal field density $\rho(0; H)$ shown by Figure 2a. The curve $\rho(0; H)$ has a sharp maximum, decreases abruptly to 0 on one side and much more smoothly on the other side. The field values which satisfy the Prokofiev-Stamp prediction for a long time correspond to the smooth side. Those which correspond to the steep side and to the maximum satisfy the Prokofiev-Stamp prediction during a shorter time. We have no precise explanation for these observations, but it seems to be related to the sharp edge of the distribution and to the fact that the spin interested by relaxation are in this case mostly concentrated on the surface of the sample.

6.2 Long time behavior

6.2.1 Spherical sample

Figure 6 shows the total magnetization at long times in the case of a sphere. It turns out to be well fitted by a stretched exponential with $\beta_1 = 0.37$; however the good agreement with (6) is not very significant since, as will be seen later, the parameter β_1 seems to depend on the sample shape, and the experiments are mostly done on a parallelepipedic sample. No good fit by (15) is possible.

The distribution $\rho(t; H)$ of the internal fields, initially very sharply peaked, smoothens as shown by Figure 7.

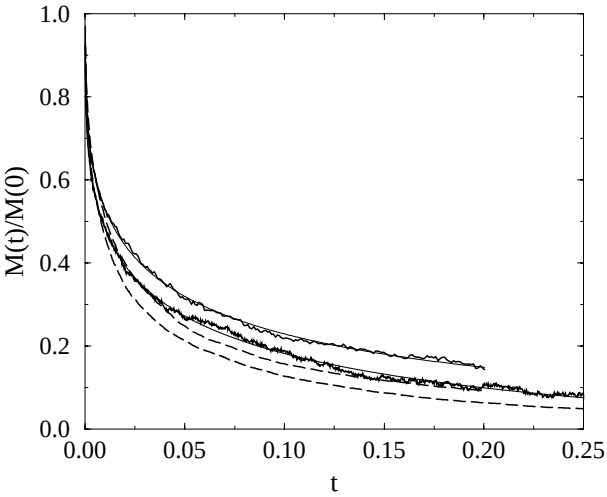

Fig. 6. Long time relaxation of the magnetization in a spherical sample of radius $r = 13$ for $\eta(0) = 10^4$. Continuous lines: magnetization as function of time for external applied field $h = 0.1$ (uppermost curve, fitted stretched exponential parameters: $\beta_1 = 0.36$, $\tau = 0.036$) and $h = 0$ (fitted stretched exponential parameters: $\beta_1 = 0.33$, $\tau = 0.037$). The dashed lines show the fraction of spins which have never flipped, for the same values of the applied field and in the same order. The thin, steady lines through the magnetization curves are the stretched exponential fits.

6.2.2 Cubic and parallelepipedic samples: effect of geometry

The magnetization of a cube is shown by Figure 8, together with the magnetization of smaller cubes of various sizes having the same center as the whole sample. The external field H is chosen such that the internal field vanishes at the center of the sample at $t = 0$, *i.e.* $H = 0$ in our model. The magnetization of the central region is seen to have almost completely vanished while the relaxation is still very weak at the periphery of the sample. This suggests that the latest stage of the relaxation is dominated by the motion of the boundary of the relaxed region.

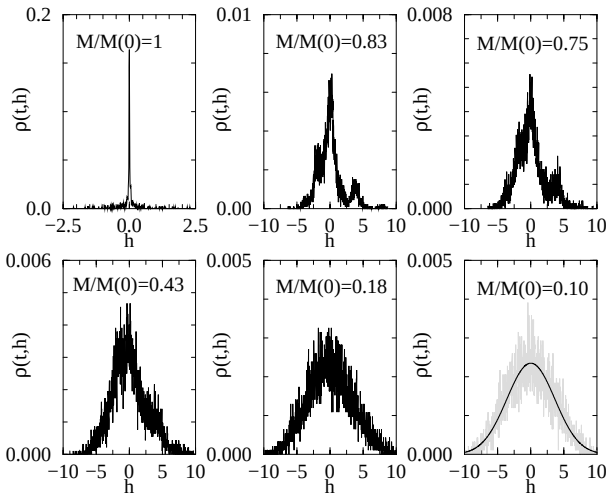

Fig. 7. Evolution of the field distribution in a sphere with no applied field; in each picture the value of the corresponding magnetization is given. The thin line in the last picture is a Gaussian fit.

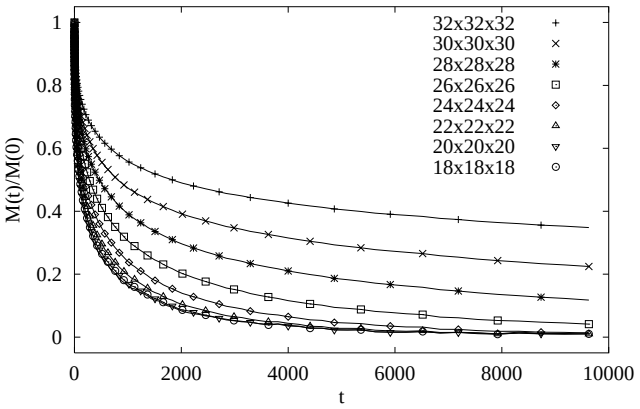

Fig. 8. Magnetization as a function of time for a cubic sample of 32^3 spins and in regions of cubic shape having the same center as the cube. The external field is chosen such that the internal field vanishes at the center of the sample at $t = 0$, $H_1 = 0.1$, $\eta(0) = 1$ (in order to compare with the data for other sample shapes reported in the other figures, please note that a change of $\eta(0)$ entails only a rescaling of time), and the average is done over 20 realizations. Upper curve: magnetization in the full sample of 32^3 spins. Lower curves: magnetization in subcubes, concentric to the full one, of the dimension given in the legend.

The cubic shape of the inner regions chosen in Figure 8 is the simplest choice, but perhaps not the best. At short times, the relaxed region is indeed expected to be the volume where the internal field vanishes in the saturated sample, and this volume is more complicated than a cube.

The relaxation of the central region is well described by the formula

$$t = A \ln^2[m(t)/s] + B \ln^3[m(t)/s] \ , \qquad (22)$$

with $B/A \approx 0.1$.

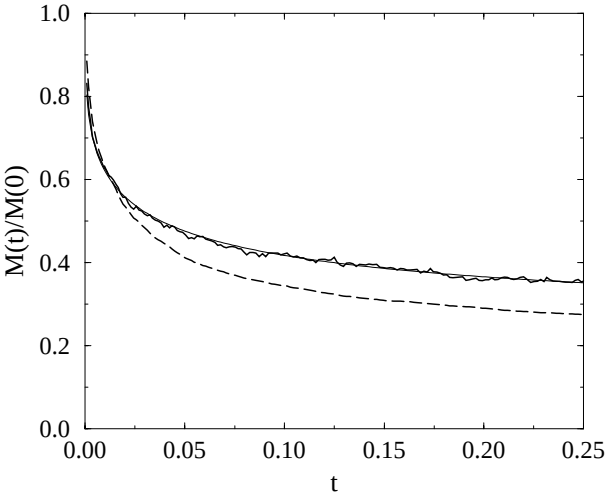

Fig. 9. Long time relaxation of the magnetization in a parallelepipedic sample $12 \times 17 \times 36$ for $\eta(0) = 10^4$ in external applied field $h = 2.4$. Continuous line: magnetization as function of time; dashed line: fraction of spins which have never flipped; the thin, steady line through the magnetization curves is the stretched exponential fit with parameters $\beta_1 = 0.33$, $\tau = 0.026$.

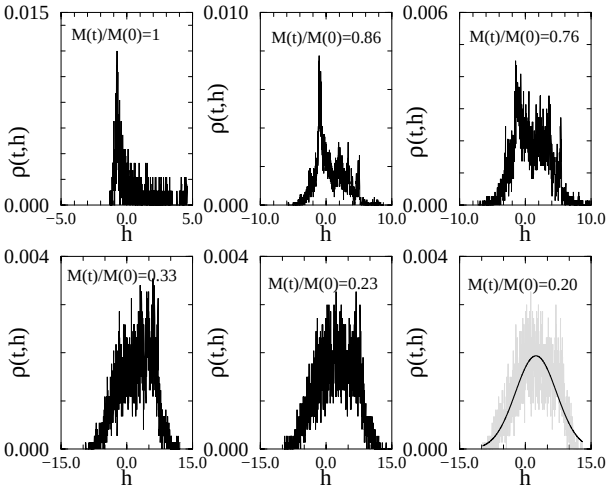

Fig. 10. Evolution of the field distribution in a parallelepiped $12 \times 17 \times 36$ with external applied field $h = 2.4$, corresponding to a local field $h_i = -0.704$ at the center of the sample; in each picture the value of the corresponding magnetization is given.

The decay of the total magnetization is very well fitted, until 0.15 times the saturation value, by a stretched exponential with $\beta_1 = 1/4$, which is quite far from the experimental value (6) for elongated samples. A simulation done in an elongated parallelepipedic sample (Fig. 9) yields $\beta_1 = 0.33$, which is closer to the experimental value.

The distribution $\rho(t; H)$ of the internal fields, initially very sharply peaked, smoothens as shown by Figure 10 in the case of a parallelepiped.

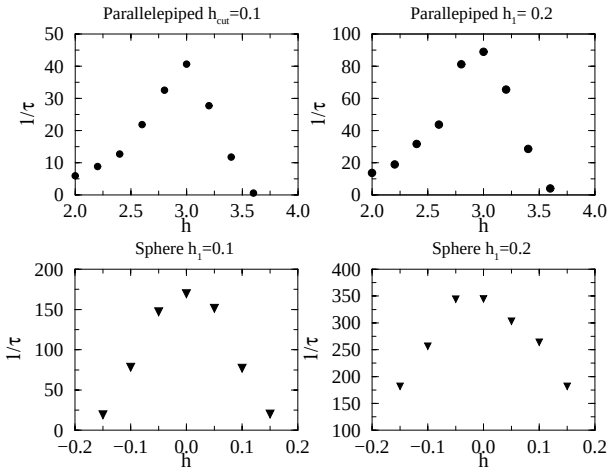

Fig. 11. Short time inverse relaxation time τ^{-1} as a function of applied field for a sphere of radius $r = 13$ (lower pictures) and a parallelepiped $12 \times 17 \times 36$ for two different widths of the resonance, $H_1 = 0.1$ (left) and $H_1 = 0.2$ (right) and $\eta(0) = 10^4$.

6.2.3 Effect of H_1

The effect of H_1 is shown by Figure 11. The time scale is modified as expected, but the dependence of the relaxation time with respect to the external field is not strongly modified, and well compares with that observed in the experiments.

7 Conclusions

Our contribution complements the work of Prokofiev and Stamp [1,2] and suggests new experiments. In particular, it is shown that the overall magnetization is remarkably well fitted by a stretched exponential, with an exponent which seems to depend on the sample shape and takes values from 1/4 to 0.4. Moreover, it is pointed out that the slow relaxation observed in parallelepipedic samples is mainly a result of the slow extension of the relaxed region, and the central region relaxes much more rapidly. The experimental check of this property would be a crucial test of the model. It might be feasible using multisquids as in the recent experiment of Wernsdorfer *et al.* [4].

Fruitful discussions with D. Gatteschi and R. Sessoli are gratefully acknowledged.

References

1. N.V. Prokofiev, P.C.E. Stamp, Phys. Rev. Lett. **80**, 5794 (1998).
2. N.V. Prokofiev, P.C.E. Stamp, J. Low Temp. Phys. **113**, 1147 (1998).
3. C. Sangregorio, T. Ohm, C. Paulsen, R. Sessoli, D. Gatteschi, Phys. Rev. Lett. **78** , 4645 (1997).
4. W. Wernsdorfer, T. Ohm, R. Sessoli, C. Paulsen, to be published (1999).
5. T. Ohm, C. Sangregorio, C. Paulsen, Eur. Phys. J. B **6**, 195 (1998).
6. F. Hartmann-Boutron, P. Politi, J. Villain, Int. J. Mod. Phys. B **10**, 2577-2637 (1996).
7. T. Ohm, Ph.D. thesis, University of Grenoble, 1998.
8. E. Adam, L. Billard, F. Lançon, Phys. Rev. E **59**, 1212 (1999).
9. K. Binder in *Monte Carlo Methods in Statistical Physics*, edited by K. Binder (Springer Verlag, 1979).